International Geology Review
Publication details, including instructions for authors and subscription information:
http://www.tandfonline.com/loi/tigr20

Geochemistry of gold deposits in the Zhangbaling Tectonic Belt, Anhui province, China

Dezhi Huang [a b], Xianying Wang [a], Xiaoyong Yang [b c], Guoming Li [a], Shiqi Huang [a], Zhen Liu [a], Zehua Peng [a] & Ruilong Qiu [d]

[a] School of Geosciences and Environmental Engineering, Central South University of China, Changsha, China

[b] State Key Laboratory of Ore Deposit Geochemistry, Institute of Geochemistry, Chinese Academy of Sciences, Guiyang, China

[c] CAS Key Laboratory of Crust-Mantle Materials and Environments, School of Earth and Space Sciences, University of Science and Technology of China, Hefei, China

[d] Geological Survey of Anhui Province, Hefei, China

Published online: 06 Jul 2010.

To cite this article: Dezhi Huang , Xianying Wang , Xiaoyong Yang , Guoming Li , Shiqi Huang , Zhen Liu , Zehua Peng & Ruilong Qiu (2011): Geochemistry of gold deposits in the Zhangbaling Tectonic Belt, Anhui province, China, International Geology Review, 53:5-6, 612-634

To link to this article: http://dx.doi.org/10.1080/00206814.2010.496225

International Geology Review
Vol. 53, Nos. 5–6, April–May 2011, 612–634

Geochemistry of gold deposits in the Zhangbaling Tectonic Belt, Anhui province, China

Dezhi Huang[a,b]*, Xianying Wang[a], Xiaoyong Yang[b,c]*, Guoming Li[a], Shiqi Huang[a], Zhen Liu[a], Zehua Peng[a] and Ruilong Qiu[d]

[a]*School of Geosciences and Environmental Engineering, Central South University of China, Changsha, China;* [b]*State Key Laboratory of Ore Deposit Geochemistry, Institute of Geochemistry, Chinese Academy of Sciences, Guiyang, China;* [c]*CAS Key Laboratory of Crust-Mantle Materials and Environments, School of Earth and Space Sciences, University of Science and Technology of China, Hefei, China;* [d]*Geological Survey of Anhui Province, Hefei, China*

(*Accepted 12 April 2010*)

The Zhangbaling Tectonic Belt (ZTB) is located in eastern Anhui province, adjacent to the Tan-Lu fault zone to the W and the Lower and Middle Yangtze River metallogenic zone to the E. Two types of gold deposits: (1) altered-tectonite gold and (2) quartz-vein gold are present in the ZTB. Three ranges of homogenization temperatures (T_h) were obtained by fluid inclusion investigations of the altered-tectonite gold deposits: 115–165°C, 235–275°C, and 335–395°C; and of the quartz-vein gold deposits: 145–195°C, 205–255°C, and 255–335°C, respectively. δD values of the ore-forming fluids range from −52.2‰ to −75.3‰, and their isotopic compositions calculated from quartz analytical data show negative $\delta^{18}O$ values (−6.3–0.1‰) for the quartz-vein gold deposits. The calculated $\delta^{18}O$ values of water are evidently lower than magmatic water, and probably were derived from mixtures of magmatic and meteoric water. Although the total rare earth elements (REE) content of the quartz-vein gold ores are much lower than those of the spatially associated granites, their chondrite-normalized patterns are similar, indicating that ore-forming elements in the ZTB quartz-vein gold deposits probably were derived from the plutons. Ores from the altered-tectonite gold deposits show δEu values and chondrite-normalized REE patterns similar to those of the granites, indicating that ore-forming elements of the altered-tectonite gold deposits also were sourced in the Yanshanian plutons. The gold deposits in the ZTB are remarkably similar to those in the Jiaodong gold metallogenic province with regard to tectonic settings, mineralization-controlling factors, mineralization ages, and the ore-forming temperatures and the stable isotopic compositions.

Keywords: gold deposits; fluid inclusion; hydrogen and oxygen isotopes; REE; Zhangbaling Tectonic Belt; east Anhui province; China

Introduction

The Zhangbaling Tectonic Belt (ZTB) is located in eastern Anhui province, which is adjacent to the Tan-Lu fault zone to the W and the Lower and Middle Yangtze River metallogenic zone to the E. This NNE–SSW-striking belt extends to Susong to the S, then westward to Wudang and Suixian in Hubei province. To the N, it extends to Guanyun in Jiangsu province

*Corresponding authors. Email: dzhuang_01@163.com; xyyang555@163.com

ISSN 0020-6814 print/ISSN 1938-2839 online

DOI: 10.1080/00206814.2010.496225
http://www.informaworld.com

(Figure 1). A rift developed in ZTB during the late Proterozoic, with acceptation of extensive marine volcanic rocks and sediments which were modified by the subsequent Triassic blueshists-facies metamorphism (Jin *et al.* 1991).

Several gold deposits are distributed in the ZTB, which are probably associated with Yanshanian granite (Huang *et al.* 2000a). Two major types, that is, mineralized tectonic breccias and gold-bearing quartz veins, can be observed in the ZTB, which commonly coexist in their occurrence. $^{40}Ar/^{39}Ar$ dating of quartz from gold deposits gave ages between 116.1 ± 0.6 Ma and 118.3 ± 0.5 Ma (Ying and Liu 2002), which shows that the gold mineralization is coeval with or slightly postdate granitoid intrusions. This can be compared with that of the Jiaodong gold province in Shandong in the N along the Tan-Lu fault zone (Chen *et al.* 2004a) and the Shaxi copper–gold deposits in the adjacent Lower Yangtze metallogenic zone (Yang *et al.* 2002). The occurrences of all major ore bodies are controlled by the sub-fractures of Tan-Lu fault zone (Zhu *et al.* 2007), indicating that the granite intrusions and the gold mineralization are closely correlated with the tectonic movement similar to the situation in Jiaodong.

The ZTB is key to connecting two famous metallogenic zones in China: the Lower and Middle Yangtze River and the Jiaodong. The study of the tectonic evolution and mineralization in the ZTB can provide valuable information for further probing into the relationship between tectonic evolution and mineralization in these two famous metallogenic zones. Meanwhile, ZTB is similar to Jiaodong in tectonic settings and mineralization-controlling factors, which shows a potential of gold mineralization in ZTB. However, study on the deposits in Zhangbaling area is still poor. This article presents data of element compositions and fluid inclusions from fresh igneous rocks and altered rocks. Discussion is focused on the origins of the ore-forming fluids and their implications for ore genesis of gold mineralization in ZTB, on the basis of oxygen- and hydrogen-stable isotopes and rare earth elements (REE). Detailed comparison is shown between gold mineralization in ZTB and the Jiaodong peninsula, the largest gold production base in China, which is also controlled by the Tan-Lu fault zone (Zhou *et al.* 2002).

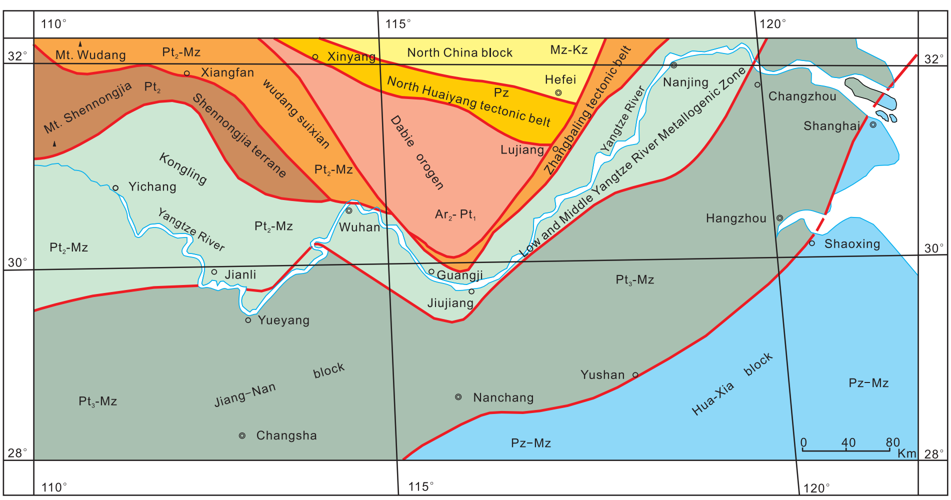

Figure 1. Tectonic map showing the situation of the Zhangbaling Tectonic Belt (modified from Dong and Huang 1995).

Geologic setting and geology of the deposits

Geologic setting

The ZTB is situated in Anhui province in China, which is adjacent to the Chu-He fault to the E and the Tan-Lu fault zone to the W. The Tan-Lu fault zone comes through the entire mineralization region and results in strong deformation in the Jurassic (Xu *et al.* 1987; Yang *et al.* 1998, 2001a). The strata exposed in the ZTB include the Neoproterozoic Zhangbaling group, the Sinian system, the lower Palaeozoic, and the Cretaceous–Palaeogene system (see Figure 2 for distributions). The Zhangbaling group is composed of schists and

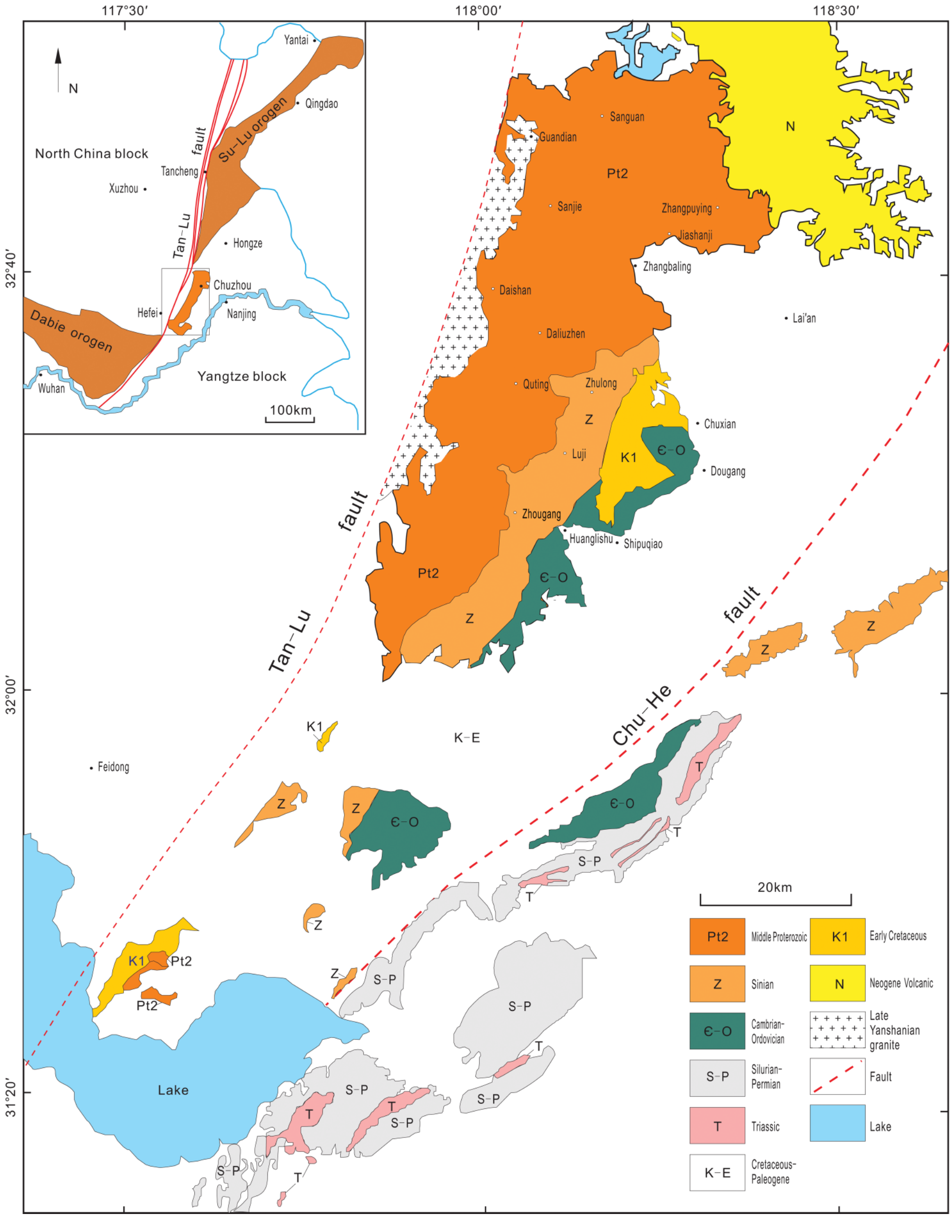

Figure 2. Schematic map of the Zhangbaling Tectonic Belt (Modified from BGMR 1987).

phyllites with banded blueschists, which were formed inside late Proterozoic aulacogen (BGMR 1987). Studies show that the metamorphism of the Zhangbaling group took place during the Triassic period (Niu *et al.* 1993). The lower Sinian system consists of clastic sedimentary rocks and the upper system mainly consists of limestone and siliceous limestone. The lower Palaeozoic unit is a sequence of shallow marine carbonates and clastic sedimentary rocks. The Cretaceous–Palaeogene rocks were dominated by fluvial and lacustrine sandstones and conglomerates with minor volcanic rocks.

The granitoid intrusions are distributed in the western part of the belt, and are adjacent and parallel to the Tan-Lu fault zone, stretched in a NNE–SSW direction (Figure 2). Gold deposits in the ZTB are widely scattered. In the Zhangbaling area, it is conspicuous that the gold mineralization, either from deposit or orebody scale, was controlled by fractures, which are part of the Tan-Lu fault system. The second-order, deep Guandian–Longwangjian fault, characterized by ductile deformation, controls the regional distribution of most gold deposits in this belt (Huang *et al.* 2000b).

Deposits geology

Quartz-vein gold deposits

The quartz-vein gold deposits in the ZTB are mainly composed of intensive quartz veins with economic gold grade. The quartz vein lodes are confined to fractures in three directions: NNW–SSE, NW–SE, and NNE–SSW. The NNE–SSW-trending lodes usually dip to the NWW in steep angles with thicknesss of 0.2–1 m. The NW–SE-trending lodes have SW dip with an average thicknesss of 0.5 m and the NNW–SSE-trending lodes dip to the SWW with thicknesss of 1–2 m.

Wall-rock alteration associated with gold mineralization is characterized by K-feldspar and silica alteration, sericitization, chloritization, carbonation, and pyritization. The ore is dominated by sulphide-bearing quartz veins. The mineral assemblage of the ore includes quartz, carbonate, albite, pyrite, arsenopyrite, sphalerite, galena, chalcopyrite, magnetite, and traces of other minerals. Gold mainly occurs as microscopic inclusions in arsenopyrite, pyrite, and chalcopyrite.

Paragenetically, the mineralization is divided into three stages: (1) an early Au-poor stage with pyrite-arsenopyrite-quartz assemblage; (2) an Au-rich stage with pyrite-arsenopyrite-chalcopyrite-galena-sphalerite-quartz assemblage; and (3) late-stage quartz-carbonate (Huang *et al.* 2000a). The fine-grained gold is mainly associated with pyrite or arsenopyrite, which is similar to the Shaxi copper-gold deposits in the adjacent Lower Yangtze metallogenic belt (Yang *et al.* 2002).

Altered-tectonite gold deposits

Mineralization in this type of gold deposit is disseminated in the altered-tectonite zone inside which structural breccia is developed. The occurrence of the ore body is concordant with and confined to the altered-tectonite zone, which is trending NNE and dipping SEE with a thickness of 2–10 m. Sulphide-bearing quartz veinlets, which formed at late-stage mineralization, can be found inside the altered-tectonite zone.

Wall-rock alteration in association with gold mineralization is intense and shows obvious alteration zoning. According to the mineral assemblages, from the centre of the tectonite zone into the wall rock, the alteration can be divided into three zones: a pyrite-quartz-sericite-chlorite zone, a sericite-quartz-chlorite zone, and a quartz-potassium feldspar zone. The ore types include altered structural breccia and minor veins inside or adjacent to the structural breccia zone. The sulphide minerals consist mainly of pyrite and arsenopyrite together with scarce amounts of chalcopyrite, sphalerite, and galena.

Petrochemistry of intrusive rocks and ore deposits

Major elements of intrusive rocks

The chemical compositions of the intrusions associated with gold mineralization in the ZTB are presented in Table 1. Some of the granitic rocks in this region are petrographically classified as quartz monzodiorite, and the others as granodiorite and granite based on the quartz-alkali feldspar-plagioclase (QAP) diagram (Figure 3), which indicates that the intrusions in this belt are mainly composed of granodiorite, quartz monzodiorite, and granite. The chemical classification of the $Na_2O + K_2O - SiO_2$ (TAS) diagram (Figure 4) shows that most samples from the area belong to subalkaline series, and are characterized by high-K value (Figure 5).

Rare earth elements of intrusive rocks

The data of REE and trace elements of intrusive rocks associated with mineralization in the ZTB are listed in Table 2. The total REE contents are between 103 and 233 ppm, with enriched light REE (LREE) relative to heavy REE (HREE) without Eu anomaly (Figure 6). The chondrite-normalized patterns of REE curves of the granitoid samples from different intrusions are similar. The $(La/Yb)_N$ ratio varied from 13.79 to 47.18. The total REE contents of granites are slightly higher than those of the granites from Jiaodong in Sangdong province (Xu *et al.* 2002), which may be because of the differences of source rocks of the granites and the degree of partial melting. The total REE contents and the chondrite-normalized patterns are similar to those of the granitoids from the Lower Yangtze metallogenic belt (Yang *et al.* 2009), which were probably derived from the lower crust (Yang *et al.* 2009).

Table 1. Analyses of major elements of granitoid intrusions from Zhangbaling Tectonic Belt.

Sample	Rocks	SiO_2	TiO_2	Al_2O_3	Fe_2O_3	FeO	FeOT	Fe_2O_3T	MnO	MgO
D-10	Quartz monzodiorite	60.77	0.73	14.79	1.81	3.58	5.21	5.79	0.09	4.33
D-9	Quartz monzodiorite	61.34	0.71	14.73	1.85	3.46	5.12	5.69	0.09	4.17
D12	Monzogranite	65.14	0.54	14.5	1.16	2.7	3.74	4.16	0.07	3.12
G-2	Quartz monzodiorite	60.84	0.81	14.32	2.13	3.45	5.37	5.96	0.1	4.73
G-6	Monzogranite	65.6	0.63	14.06	1.58	2.74	4.16	4.62	0.09	3.06
S-1	Quartz monzodiorite	62.5	0.64	15.45	1.9	2.95	4.66	5.18	0.1	3.43
ZK51-6	Granite	68.42	0.4	14.14	1.23	11.86	12.97	14.41	0.05	1.96
ZK53-5	Granite	65.76	0.48	14.3	1.66	2.01	3.5	3.89	0.06	2.58
Sample	Rocks	CaO	MgO	CaO	Na_2O	K_2O	P_2O5	H_2Op	CO_2	Total
D-10	Quartz monzodiorite	4.88	4.33	4.88	3.86	3.36	0.34	0.79	0.25	99.58
D-9	Quartz monzodiorite	4.63	4.17	4.63	3.81	3.4	0.33	0.79	0.25	99.49
D12	Monzogranite	3.56	3.12	3.56	3.56	3.7	0.22	1.08	0	99.57
G-2	Quartz monzodiorite	5.26	4.73	5.26	3.88	3.15	0.34	0.6	1.67	99.61
G-6	Monzogranite	3.63	3.06	3.63	3.5	4	0.25	0.75	0	99.89
S-1	Quartz monzodiorite	4.09	3.43	4.09	4.79	2.03	0.26	1.21	0.67	100.02
ZK51-6	Granite	2.6	1.96	2.6	3.77	4.1	0.02	0.73	0.23	99.5
ZK53-5	Granite	3.23	2.58	3.23	4.02	3.85	0.19	0.83	0.74	99.71

Source: From Li *et al.* 1985.

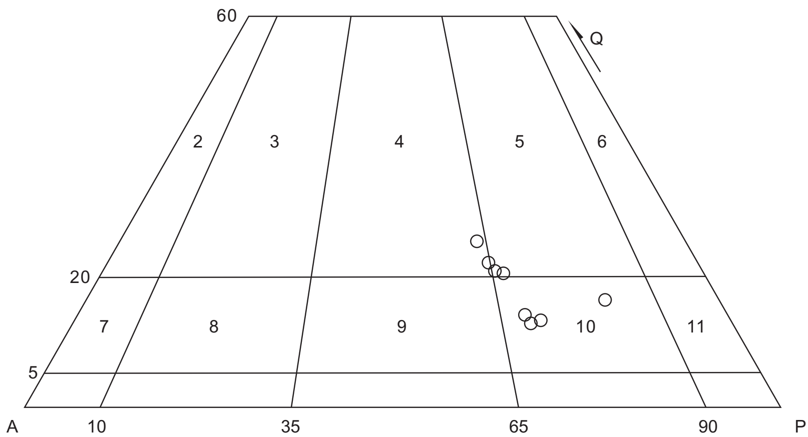

Figure 3. The QAP diagram of granitoid intrusions in the Zhangbaling Tectonic Belt. 2, Alkali-feldspar granite; 3, potassium-feldspar granite; 4, monzonitic granite; 5, granodiorite; 6, tonalite; 7, alkali-feldspar quartz syenite; 8, quartz syenite; 9, quartz monzonite; 10, quartz monzodiorite; 11, monzodiorite.

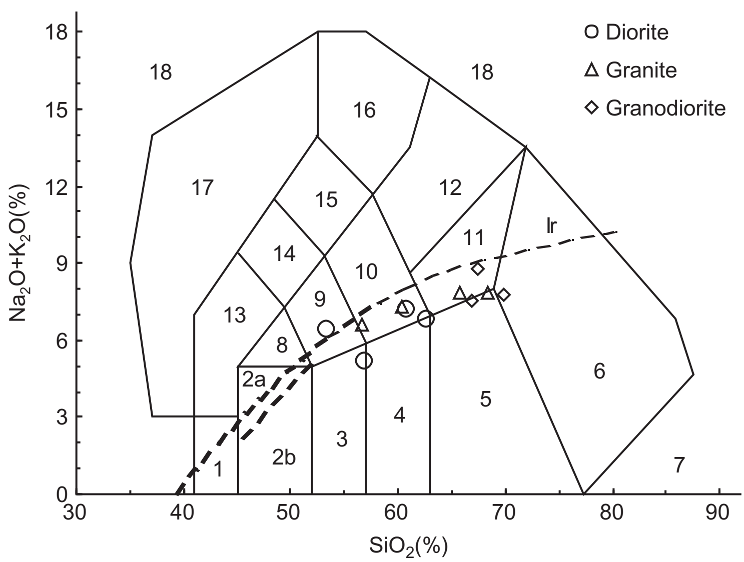

Figure 4. Chemical classification of the TAS diagram (Wilson 1989). 1, olive gabbro; 2a, Syenogabbro; 2b, gabbro; 3, gabbro-diorite; 4, diorite; 5, granodiorite; 6, granite; 8, alkali-gabbro; 9, alkali-gabbroicdiorite; 10, syenodiorite; 11, alkali-grnnodirite; 12, syenite; 13, feldspathoid gabbro; 14, feldspathoid monzonite diorite; 15, feldspathoid menzonitic syenite; 16, feldspathoid syenite; 17, foidite pluton; 18, leucite rock.

Rare earth elements of golde deposits

REE of quartz-vein gold deposits

To trace the origin of the ore-forming elements of the quartz-vein gold deposits in the ZTB, the ore samples in quartz-vein gold deposits were collected for REE analysis as well (see Table 2). The total REE contents of the ores, both fresh and oxidized, are much lower

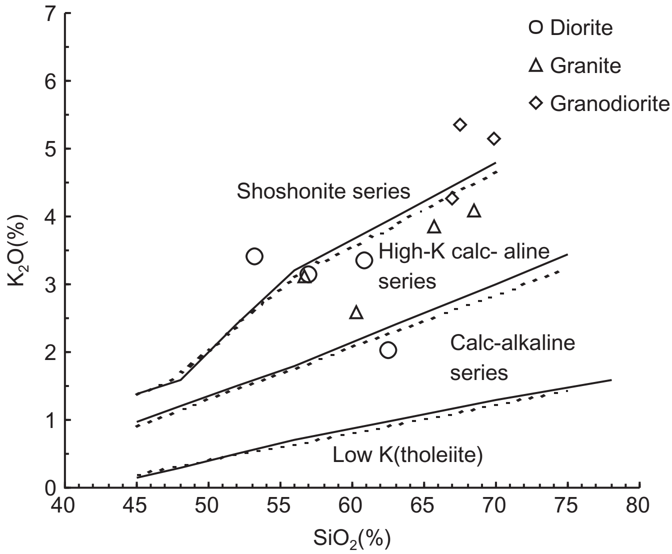

Figure 5. SiO_2–K_2O diagram for the granitoid rocks in the Zhangbaling area (after Le Maitre *et al.* 1989; Rickwood 1989).

than those of granites. This probably indicates that REEs tend to incorporate into granites rather than the ore-forming fluids. However, the chondrite-normalized patterns of REE curves of granites and fresh ores are similar (Figure 7). The $(La/Yb)_N$ is from 10.45 to 22.92, which shows that the samples are rich in LREEs as seen from the curves. The chondrite-normalized patterns of REE curves of oxidized ores display different patterns from those of granites and fresh ores. The oxidized ores are relatively rich in HREEs, which may be because of the release of LREEs during oxidation, whereas HREEs are relatively stable and tended to remain inside oxidized ores. Therefore, the results of REEs, especially the similar chondrite-normalized patterns of granites and ores, indicate that the ore-forming elements of quartz-vein gold deposits in the Zhangbaling are possibly derived from Yanshanian granites.

REEs of altered-tectonite gold deposits

Wall-rock alteration in association with gold mineralization in mineralized altered tectonites is more intense and shows more evident alteration zoning in the study region, which implies that the ore-forming fluid flow is not limited to ore-bearing structural conduits, but instead involves interaction between auriferous fluids and surrounding host rocks. Therefore, it cannot be excluded that the wall rocks supply partly ore-forming elements. To probe into the relationship between wall rock and mineralization, the REEs of granites and ores, as well as altered tectonite and wall rock were analysed (see Table 2). The total REE contents of granite just adjacent to ore, altered wall-rock, tectonite, and ore range between 219.14 and 234.31 ppm. However, the differences of the chondrite-normalized patterns of REE curves between these four types of samples are obvious, especially on the LREE pattern curves and δEu (Figure 8).

The $(Ce/Yb)_N$ ratios of granites, ore, altered tectonite, and wall rock are 20.81, 8.90, 5.05, and 4.13, respectively, which display the relative increase in HREEs in the order

Table 2. The REE and trace element data of granitoids and gold deposits from Zhangbaling.

Sample	Rocks	La	Ce	Pr	Nd	Sm	Eu	Gd	Tb	Dy	Ho	Er	References
D6	Diorite	38.6	76.08	9.75	38.14	6.92	1.98	5.85	0.79	3.98	0.71	1.78	This study
D10	Diorite	35.24	66.81	7.77	27.18	4.62	1.32	3.47	0.49	2.58	0.49	1.32	This study
S-1	Diorite	25.92	55.08	7.14	27.5	4.74	1.42	3.52	0.47	2.46	0.48	1.35	This study
ZK51-6	Granite	29.81	52.48	5.53	18.24	2.91	0.8	1.99	0.3	1.52	0.29	0.73	This study
Zk53-5	Granite	21.88	46.49	5.31	18.72	3.14	0.86	2.36	0.35	1.77	0.35	0.93	This study
Zk92-4	Granite	57.95	106.9	12.12	39.55	6.14	1.66	4.01	0.53	2.39	0.44	1.07	This study
Zk92-6	Granite	52.65	97.07	10.79	37.88	6.05	1.65	4.53	0.62	3.12	0.57	1.42	This study
WWL-1	Granodiorite	31.21	53.78	5.1	18.06	2.39	2.01	2.67	0.35	1.28	0.28	0.85	Niu et al. (2002)
WWX-1	Granodiorite	25.54	49.7	5.44	19.71	3.35	1.22	2.88	0.38	1.74	0.33	0.93	Niu et al. (2002)
AGD-1	Granodiorite	32.99	55.73	5.44	19.01	3.98	1.76	2.93	0.31	1.65	0.31	1.08	Niu et al. (2002)

Sample	Rocks	Tm	Yb	Lu	Y	ΣREE	LREE	HREE	LREE/HREE	La_N/Yb_N	δEu	δCe	References
D6	Diorite	0.27	1.41	0.22	19.74	186.48	171.47	13.11	11.42	18.50	0.95	0.92	This study
D10	Diorite	0.22	1.17	0.19	13.06	152.87	142.94	8.35	14.39	20.35	1.01	0.95	This study
S-1	Diorite	0.21	1.27	0.18	13.26	131.74	121.80	8.28	12.25	13.79	1.06	0.95	This study
ZK51-6	Granite	0.13	0.74	0.12	7.6	115.59	109.77	4.83	18.86	27.22	1.02	0.96	This study
Zk53-5	Granite	0.16	1.01	0.17	9.78	103.50	96.40	5.76	13.58	14.64	0.97	1.01	This study
Zk92-4	Granite	0.18	0.83	0.14	11.036	233.91	224.32	8.44	23.39	47.18	1.02	0.95	This study
Zk92-6	Granite	0.23	1.19	0.19	14.76	217.96	206.09	10.26	17.36	29.90	0.96	0.95	This study
WWL-1	Granodiorite	0.08	0.68	0.09	8.15	118.83	112.55	5.43	17.92	31.01	2.43	1.00	Niu et al. (2002)
WWX-1	Granodiorite	0.15	0.88	0.14	8.97	112.39	104.96	6.26	14.13	19.61	1.20	0.99	Niu et al. (2002)
AGD-1	Granodiorite	0.09	0.79	0.09	8.2	126.16	118.91	6.28	16.40	28.22	1.58	0.97	Niu et al. (2002)

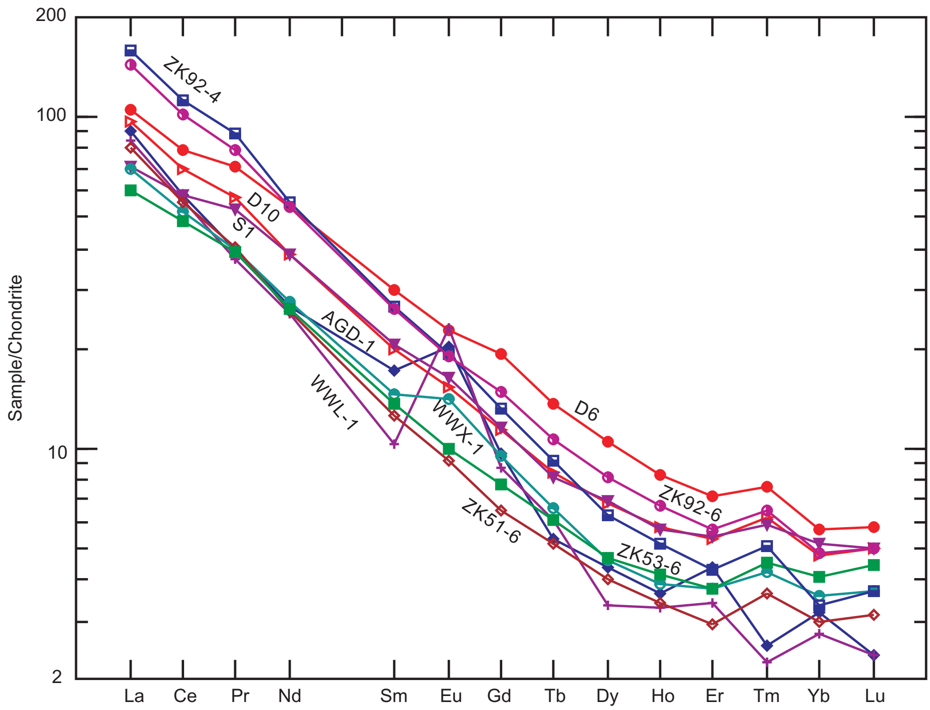

Figure 6. Chondrite-normalized REE distribution patterns of the granitoids in the Zhangbaling.

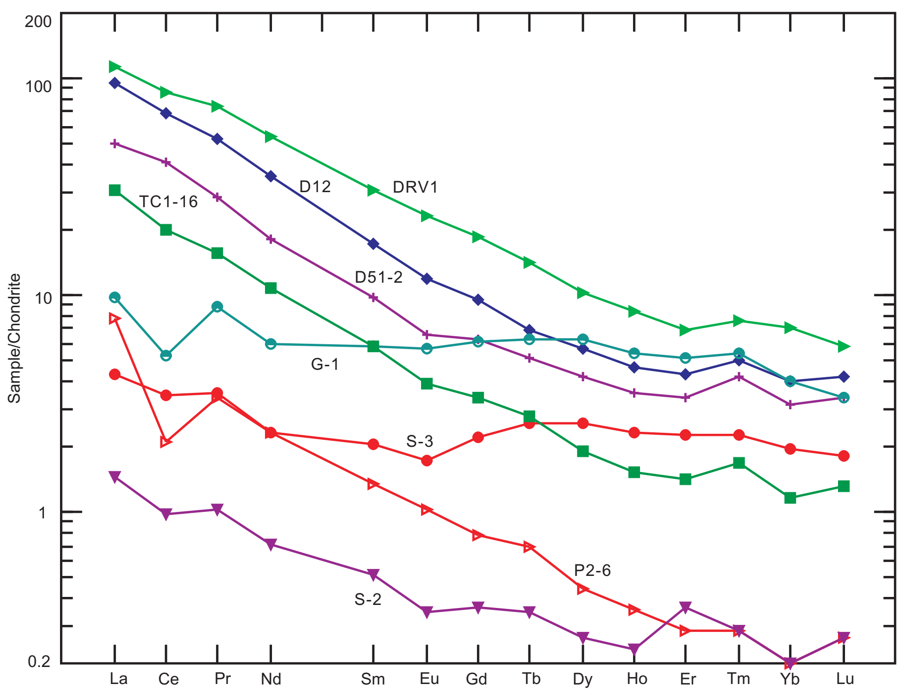

Figure 7. Chondrite-normalized REE patterns of the granites and ores in quartz-vein gold deposits.

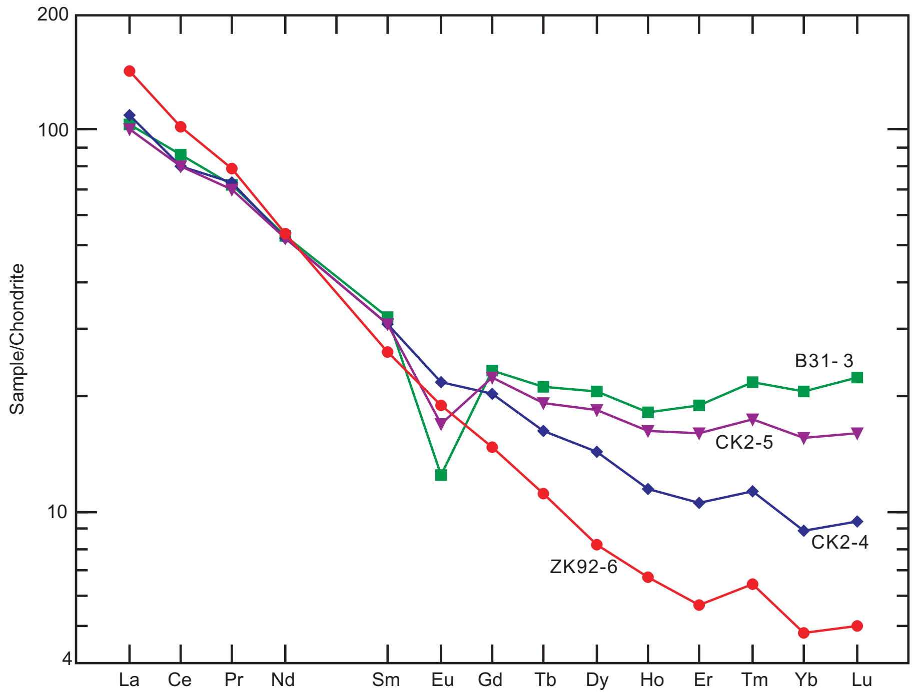

Figure 8. Chondrite-normalized REE patterns of the granites and ores in altered-tectonite gold deposits.

granites > ore > altered tectonite > wall rock. The δEu values of granites, ore, altered tectonite, and wall rock are 0.93, 0.86, 0.64, and 0.45, respectively, which display the increase in Eu depletion from granites to ore, altered tectonite, and wall rock. As a whole, the chondrite-normalized patterns of REE curves of granites and ore are similar, which indicates that ore-forming elements of altered-tectonite gold deposits in Zhangbaling are from Yanshanian granites, the same as those of quartz-vein gold deposits. The pattern of the REE curve of altered tectonite is similar to wall rock and tends to approach the curves of ore and granite, which implies that the REEs in altered tectonite mainly inherit from wall rock, and take in partly those from ore-forming fluids originating from granites.

The ore-forming fluids

Temperature and salinity of fluid inclusions

Microthermometric measurements of primary fluid inclusions in quartz samples from the Guodawa, Songweizi, Tonggoucheng, and Xiaomiaoshan were conducted using the Linkam THMSG-600 programmed heating–freezing stage and employing standard procedures (Shepherd *et al.* 1985) by Yichang Institute of Geology and Resources (Table 3). It can be seen from Table 3 that most of the investigated primary fluid inclusions are composed of two phases (liquid-H_2O and vapour-H_2O). Three phases (liquid-H_2O+vapour-H_2O+vapour-CO_2) are observed only in two samples, which is different from those from the Linglong gold deposit (Shandong province), where the fluid inclusions are rich in CO_2 (Zhang *et al.* 2007). Generally, in gold deposits associated with intrusions, the early-stage ore fluids are characterized by being CO_2-rich and late-stage fluids by being CO_2-poor and

Table 3. The results of microthermometric measurements of fluid inclusions in quartz from the deposits in Zhangbaling Tectonic Belt.

Types of gold deposits	Sample number	Phases	Vapour/liquid ratios	T_h (°C)	Salinity (wt.%)
Quartz-vein gold deposits	D25	$LH_2O + VH_2O$	10–15%	165–195°C	5.4–5.7
			20–30%	255–335°C	5.8–6.7
	D51-2	$LH_2O + VH_2O$	10–15%	145–185°C	9.5–10
			15–20%	215–235°C	9–9.2
	D52-1	$LH_2O + VH_2O$	10–15%	145–195°C	8.4–8.6
			15–20%	205–255°C	8.9–9.2
	G_3	$LH_2O + VH_2O$	15–25%	205–275°C	8.6–9.2
		$LH_2O + LCO_2 \pm VCO_2$	CO_2 = 40%	275–295°C	9.84–10.58
	D_7	$LH_2O + VH_2O$	10–15%	145–195°C	11–11.8
			15–20%	205–245°C	11.97–11.29
			25–30%	275–295°C	
Altered-tectonite gold deposits	D_8	$LH_2O + VH_2O$	10–15%	115–165°C	10–11
			20–25%	265–275°C	11.1–10.6
		$LH_2O + LCO_2 \pm VCO_2$	CO_2 = 35–40%	235–245°C	11.1–10.6
			CO_2 = 60–65%	335–395°C	
			CO_2 = 75–80%	385–395°C	

the lack of daughter minerals (Yang and Zhou 2000; Yang *et al.* 2001b; Qiu *et al.* 2002; Chen *et al.* 2004b, 2007a). Therefore, the low content of CO_2 in the fluid inclusions in the Zhangbaling area may be because most of the studied fluid inclusions are formed at the late stage.

Three ranges of homogenization temperatures (T_h) were obtained by fluid inclusion investigations of the altered-tectonite gold deposits: 115–165°C, 235–275°C, and 335–395°C, and of the quartz-vein gold deposits: 145–195°C, 205–255°C, and 255–335°C, respectively (Table 3 and Figure 9), which shows that the two types of gold deposits were formed under similar temperatures except that the former show slightly higher temperature on high-temperature range, and the later are closer to those obtained from Jiaodong in the Shandong province (Chen *et al.* 2004b, 2007a). The T_h of the fluid inclusions in the samples from quartz-vein gold deposits are similar to most hydrothermal deposits elsewhere (e.g. Shelton and Lofstro 1988; So *et al.* 1997; Xie *et al.* 2009).

The salinity of the two-phase (liquid-H_2O and vapour-H_2O) fluid inclusions from quartz-vein gold deposits range between 5.4 and 9.2 wt.% NaCl equivalent and the corresponding T_h from 165°C to 275°C (see Table 3), which can be compared with inclusions trapped during the late stage in the Linglong gold deposits in Jiaodong (Zhang *et al.* 2007). The T_h of three-phase fluid inclusions (liquid-H_2O+vapour-H_2O+vapour-CO_2) in the samples from quartz-vein gold deposits range from 275°C to 295°C with a salinity ranging from 9.84 to 10.58 wt.% NaCl equivalent, whereas the salinity of three-phase fluid inclusions (liquid-H_2O+vapour-H_2O+vapour-CO_2) in the samples from altered-tectonite gold deposits are from 10.6 to 11.1 wt.%, which are similar to the middle stage from Jiaodong in Shandong province (Zhang *et al.* 2007).

H–O Stable isotopes

Stable isotope analyses (δD and $\delta^{18}O$) of minerals and fluids provide valuable insights into fluid sources, hydrothermal processes, and fluid–rock interaction in a wide range of

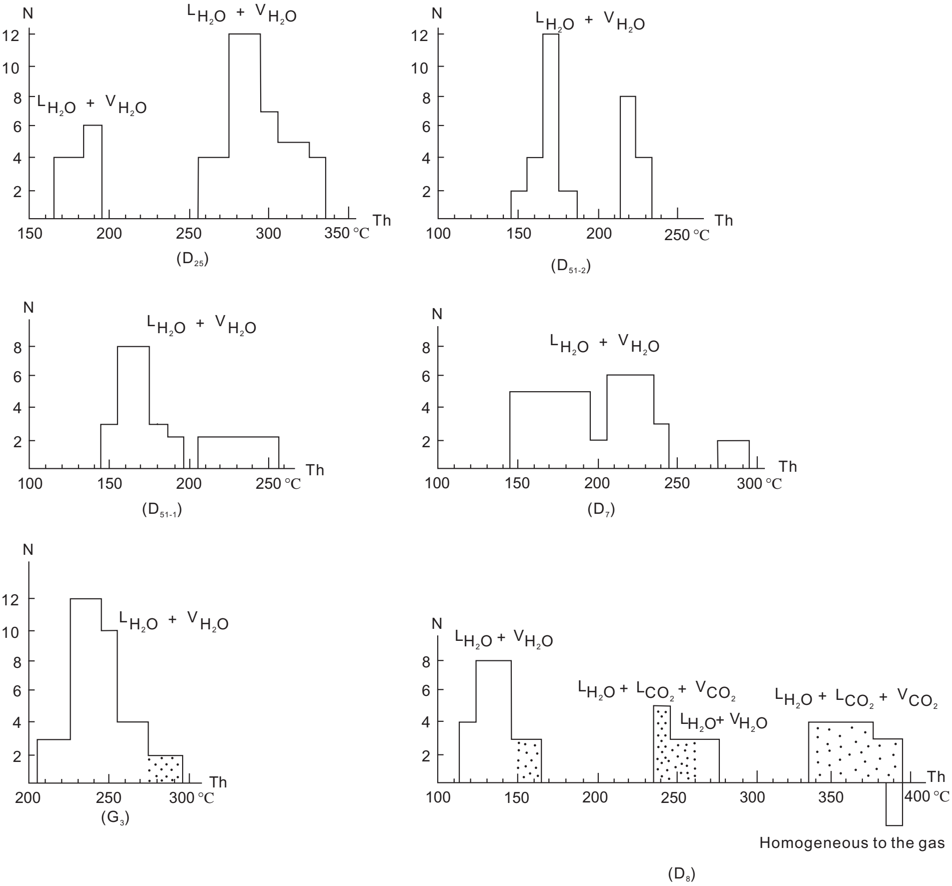

Figure 9. Homogenization temperature histograms of fluid inclusions in quartz from the deposits in the Zhangbaling Tectonic Belt.

geological environments (Wilkinson *et al.* 1995; O'Reilly *et al.* 1997; Naden *et al.* 2003). To probe the origin of ore-forming fluids in the gold deposits in the ZTB, five quartz-vein samples associated with gold mineralization are collected from quartz-vein gold deposits. Quartz was crushed into grains with sizes of 0.2–0.4 mm, and then purified more than 99% by hand-picking under a binocular microscope. Oxygen isotope compositions of separated quartz were analysed. $^{18}O/^{16}O$ ratios were measured with a MAT-261 mass spectrometer in the Isotope Laboratory of Yichang Institute of Geology and Resources of China. Oxygen was extracted from quartz by reaction with BrF_5 and converted to CO_2 by reaction with heated carbon. The ratios are reported in standard δ-notation in per mil (‰) relative to the V-SMOW standard. The accuracy of analysis is better than ±0.2‰ for $\delta^{18}O$. Two standard quartz samples, National Standard of China GBW-04409 (+11.2‰ for $\delta^{18}O$) and International Standard NBS-28 (+9.6‰ for $\delta^{18}O$), were used for reference in oxygen isotope analysis. All quartz grains used for analyses of δD of fluid inclusions were heated under vacuum at 150°C overnight to remove adsorbed atmospheric water. The resultant H_2O was reduced to H_2 by reaction with zinc metal at 500°C for 15 minutes. The δD values of the hydrogen were then measured on a MAT-261 mass spectrometer with internal biotite (δD: −64 ± 5.0‰) and kaolinite (δD: −125 ± 5.0‰) standards calibrated against the certified international biotite standard NBS-20 (δD: −65‰). The overall analytical precision for the hydrogen isotope measurements is around ±5.0‰. All results are reported in standard δ-notation in per mil (‰) relative to the V-SMOW standard.

The analysed $\delta^{18}O$ of quartz ($\delta^{18}O_q$), δD of fluid inclusions (δD_{H_2O}), and the $\delta^{18}O$ values of fluids ($\delta^{18}O_{H_2O}$) calculated by the $\delta^{18}O_q$ using the fractionation equation of Zhang (1989) and average T_h of each sample are shown in Table 4. δD values of ore-forming fluids (δD_{H_2O}) range from −52.2‰ to −75.3‰, which is similar to the δD values of fluids at the early and late stages from Shanggong gold deposit (Henan province), where the ore-forming fluid is relatively poor in D, which is due to the large-scale precipitation of sulphides (Chen *et al.* 2004b). The $\delta^{18}O$ values of quartz range from +6.4‰ to +12.1‰. The isotope compositions of the fluid calculated from the quartz data show negative $\delta^{18}O$ values, ranging from −6.3‰ to 0.1‰. The calculated $\delta^{18}O$ values of water are evidently lower than that of fluids originating from magma (+5‰ to +7‰, Sheppard 1986).

On the diagram of $\delta^{18}O_{H_2O}$ versus δD_{H_2O}, the plots of the samples are far away from the magmatic water and meteoric water (Figure 10). Hydrothermal alteration of the rocks

Table 4. Oxygen and hydrogen isotope values for samples from the Zhangbaling and Jiaodong gold deposits.

Sample order	Sample	Locality	$\delta^{18}O_Q$ (SMOW)	δD_{H_2O} (SMOW)	$\delta^{18}O_{H_2O}$ (SMOW)	References
1	D_7	Zhangbaling	10.8	−52.2	−1.3	This article
2	$D_{51\text{-}2}$	Zhangbaling	6.4	−75.3	−6.3	This article
3	G_3	Zhangbaling	9.5	−70.4	0.1	This article
4	D_{521}	Zhangbaling	12.1	−63.7	0	This article
5	D_{25}	Zhangbaling	6.6	−56.6	−1.1	This article
6	SS-435-1	Sansandao		−52	7.55	Mao *et al.* (2005)
7	SS-70-13	Sansandao		−48	8.55	Mao *et al.* (2005)
8	SS-375-4	Sansandao		−52	8.85	Mao *et al.* (2005)
9	SS-375-7	Sansandao		−53	6.55	Mao *et al.* (2005)
10	SSD1	Sansandao		−50	7.75	Mao *et al.* (2005)
11	SSD3	Sansandao		−67	7.85	Mao *et al.* (2005)
12	JJ-190-2	Jiaojia		−62	7.25	Mao *et al.* (2005)
13	JJ-190-13	Jiaojia		−86	4.37	Mao *et al.* (2005)
14	JJ-190-14	Jiaojia		−85	4.17	Mao *et al.* (2005)
15	Jjiao1	Jiaojia		−59	7.75	Mao *et al.* (2005)
16	Jjiao2	Jiaojia		−59	5.25	Mao *et al.* (2005)
17	LN-20	Linnan		−84	−4.6	Lu *et al.* (1999)
18	LN-18	Linnan		−85	−4.8	Lu *et al.* (1999)
19	95LN-1	Linnan		−86	−7.4	Lu *et al.* (1999)
20	LL-190-12	Linlong		−59	2.6	Mao *et al.* (2002)
21	LL-190-122	Linlong		−68	2.4	Mao *et al.* (2002)
22	LL-190-1	Linlong		−61	2.6	Mao *et al.* (2002)
23	LL-190-111	Linlong		−72	2.5	Mao *et al.* (2002)
24	LL-190-2	Linlong		−76	3.6	Mao *et al.* (2002)
25	D22-3	Dazhuangzi		−62	−2.2	Mao *et al.* (2002)
26	D22-4	Dazhuangzi		−70	−3	Mao *et al.* (2002)
27	D22-5	Dazhuangzi		−57	−6.5	Mao *et al.* (2002)
28	D22-6	Dazhuangzi		−72	−7.4	Mao *et al.* (2002)

Note: $\delta^{18}O_Q$:$\delta^{18}O$ values of quartz; δD_{H_2O}:δD values of water; $\delta^{18}O_{H_2O}$:$\delta^{18}O$ values of water, calculated from the quartz analyses using the fractionation equation $1000\ \ln\alpha_{quartz\text{–}water} = 3.306 \times 10^6\ T^{-2} - 2.71$ of Zhang (1989) and fluid inclusion homogenization temperatures for each quartz sample.

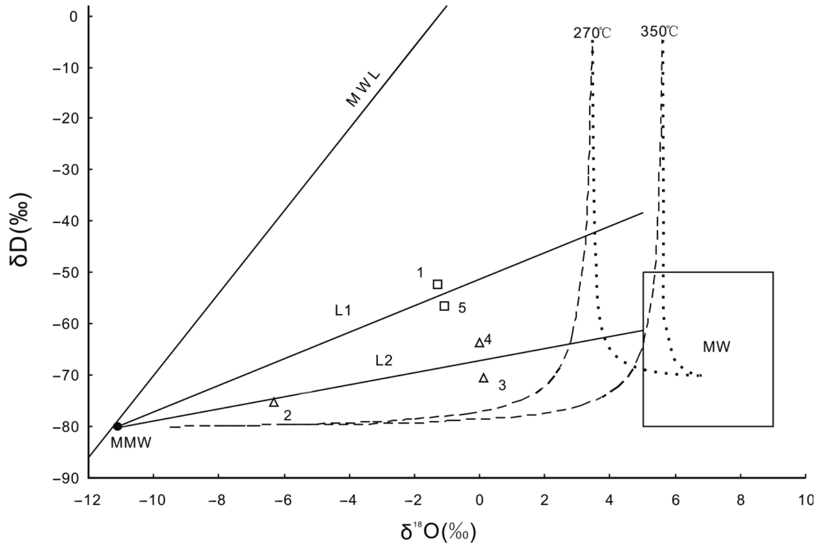

Figure 10. The $\delta^{18}O_{H_2O}$ versus δD_{H_2O} plot showing the isotopic composition of ore-forming fluids of the gold deposits in the Zhangbaling area. (MWL, meteoric water line; MMW, Mesozoic meteoric water in Zhangbaling; MW, initial magmatic water; dashed line, the change of δD and $\delta^{18}O$ values of Mesozoic meteoric water by reaction with granite in different water/rock ratios; dotted line, the change of δD and $\delta^{18}O$ values of initial magmatic water by reaction with granite in different water/rock ratios; $\delta^{18}O$ and δD values of granite as +9‰ and −70‰; $\delta^{18}O$ and δD values of initial magmatic water as +7‰ and −70‰, respectively; $\delta^{18}O$ and δD values of Mesozoic meteoric water as −11‰ and -80‰, respectively (Zhang 1989); the fractionation equations of oxygen and hydrogen between rock and water are following Zhang (1989): $1000\ln^{\alpha}{}_{pl-water} = 2.68 \times 10^6\ T^{-2} - 3.53$ and $1000\ln^{\alpha}{}_{Bi-water} = -21.3 \times 10^6\ T^{-2} - 2.8$).

is widely developed in the gold deposits in the Zhangbaling area, which suggests that the ore-forming fluids of the gold deposits may be affected by water–rock interaction. Therefore, we also modelled the isotope evolution lines of magmatic water and meteoric water through equilibrium of isotopic exchange with the granite at 270°C (about middle T_h of inclusions) and at 350°C (about the highest T_h) (Figure 10). However, the plots of the samples are not nearby the evolution lines as well. Considering the close relationship between the gold deposits and the granites in study area, the most reasonable source of ore-forming fluids for samples 1 and 5 is mixture of Mesozoic meteoric water and the evolved magmatic water, whereas the ore-forming fluids of samples 2, 3, and 4 may involve Mesozoic meteoric water, the evolved magmatic water, and initial magmatic water. Therefore, data of oxygen and hydrogen isotopes show that the ore-forming fluids of gold deposits in the ZTB are from at least two sources: Mesozoic meteoric water and magmatic water.

To compare gold deposits in Zhangbaling with those in Jiaodong, we listed some $\delta^{18}O_{H_2O}$ and δD_{H_2O} values from Jiaodong gold deposits in Table 4 as well. The oxygen and hydrogen isotopes compositions of the ore-forming liquids of Sanshandao and Jiaojia gold deposits are similar to magma-originated water. On the diagram of $\delta^{18}O_{H_2O}$ versus δD_{H_2O} (Figure 11), the plots are inside or near the scope of magmatic water. However, the $\delta^{18}O_{H_2O}$ and δD_{H_2O} values of the samples from Linglong, Lingnan, and Dazhuangzi gold deposits are deviated from that of magmatic water. The samples from Linglong and Lingnan

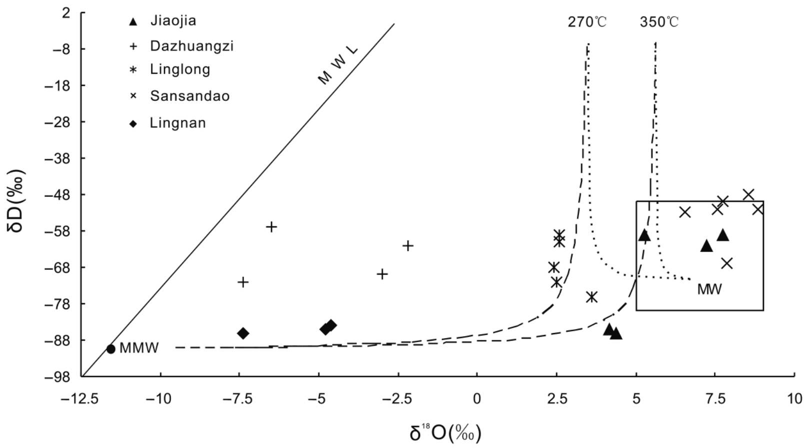

Figure 11. The $\delta^{18}O_{H_2O}$ versus δD_{H_2O} plot showing the isotopic composition of ore-forming fluids of the gold deposits in Jiaodong (data are from Lu *et al.* 1999; Mao *et al.* 2002, 2005); the symbols are the same as in Figure 10, except the $\delta^{18}O$ and δD values of Mesozoic meteoric water are –12.5‰ and –90‰ (Zhang 1989), respectively.

deposits are near the evolution lines of meteoric water through isotopic exchange with the granite at 270°C or at 350°C (Figure 11), but the plots of the samples from the Dazhuangzi gold deposit are neither inside magmatic water scope nor near the evolution lines of meteoric water. In general, the source and evolution of ore-forming fluids of Linglong, Lingnan, and Dazhuangzi gold deposits are similar to those in the Zhangbaling area to some extent.

Tectonic environment of magmatism in ZTB

Age of intrusive rocks

In the Zhangbaling area, several stages of structural deformation can be identified after the Neoproterozoic (Hou *et al.* 2004; Mercier *et al.* 2007). Among these tectonic activities, the Mesozoic fracturing movements, which are dominated by the Tan-Lu fault zone, are directly associated with gold mineralization. It is suggested that the first sinistral displacement of the Tan-Lu fault zone happened in the latest Middle Triassic, from 236.2 ± 0.5 Ma to 238.0 ± 0.4 Ma (Zhang *et al.* 2008). In the Early Cretaceous (120–130 Ma), the fault zone underwent another sinistral displacement, followed by extensional activities (Zhu *et al.* 2001a, 2001b). The recent results show that the granites in the ZTB also emplaced during this period. Niu *et al.* (2008) obtained ages of 126.9 ± 1.0 Ma, 114.8 ± 1.3 Ma, 108.1 ± 1.6 Ma, 103.0 ± 0.9 Ma, and 120.3 ± 0.7 Ma for different granitoids in the Zhangbaling by zircon U-Pb LA-ICP-MS analyses, which is concordant with the results by Liu *et al.* (2002) and Niu (2006). U-Th-Pb dating of zircons from the Guandian granite obtained an age of 128 Ma (Li *et al.* 1985). All the dating results indicate that these rocks formed in the Yanshanian period, about 20–30 million years younger than the forming ages of some important Cu-Au deposits such as Shaxi and the Tongling region in the western side of the ZTB (e.g. Mao *et al.* 2006; Yang *et al.* 2007; Xie *et al.* 2009), but coeval with the sinistral displacement of the Tan-Lu fault zone, which may record the subduction of west Pacific plate from northeast to mainland China (Sun *et al.* 2007; Lan *et al.* 2009).

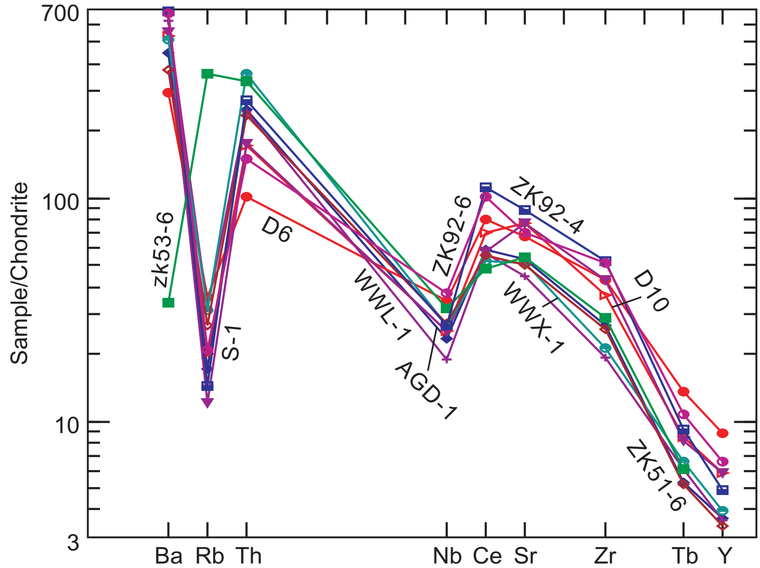

Figure 12. Spider diagrams of trace elements of granitoids in the Zhangbaling.

Origin of intrusive rocks

The I_{Sr} of the granitoids in the Zhangbaling ranges from 0.70623 to 0.70685, slightly higher than mantle source (Niu *et al.* 2002). However, the extremely high negative εNd (−15.5, Li *et al.* 1985; −16.8 to −18.1) and the low $^{206}Pb/^{204}Pb$ (16.504) and $^{207}Pb/^{204}Pb$ (15.292) ratios (Li *et al.* 1985) strongly suggested that the granites are from melting of lower crust. The result of trace elements (Figure 12) shows that among the incompatible and middle-incompatible elements, Ba and Sr are enriched evidently but Rb and Nb are relatively depleted. This may be because granitoids originated from the melting of lower-crust source rocks, which is usually rich in Ba and Sr, and relatively poor in Rb and Nb.

Tectonic environment of intrusive rocks

On the Nb–Y trace element discrimination diagram (Figure 13a), the granitoids in the Zhangbaling are located in syn-collision or volcanic arc fields, whereas on the Rb–Y + Nb diagram (Figure 13b), all the samples fall inside volcanic arc scope, which resulted from the low contents of Rb. We suggested that the granitoids in the Zhangbaling area are from melting of lower crust during or post-orogenic process, which is concordant with the conclusion from the result of Nd and Pb data (Li *et al.* 1985). Considering these rocks distributing in orogen regions associated with continent–continent collision, these high-K calc-alkaline granitoids probably indicate the change of tectonic environment from compression to extension (Xiao *et al.* 2002), similar to the situation in the Jiaodong.

Discussion of ore genesis

Orogenic gold deposits occurring in metamorphic belts have attracted interest from both researchers and industry globally (Chen *et al.* 2004b). Many researchers diagnose the orogenic gold deposits according to the sources of metals and fluids based on stable isotope

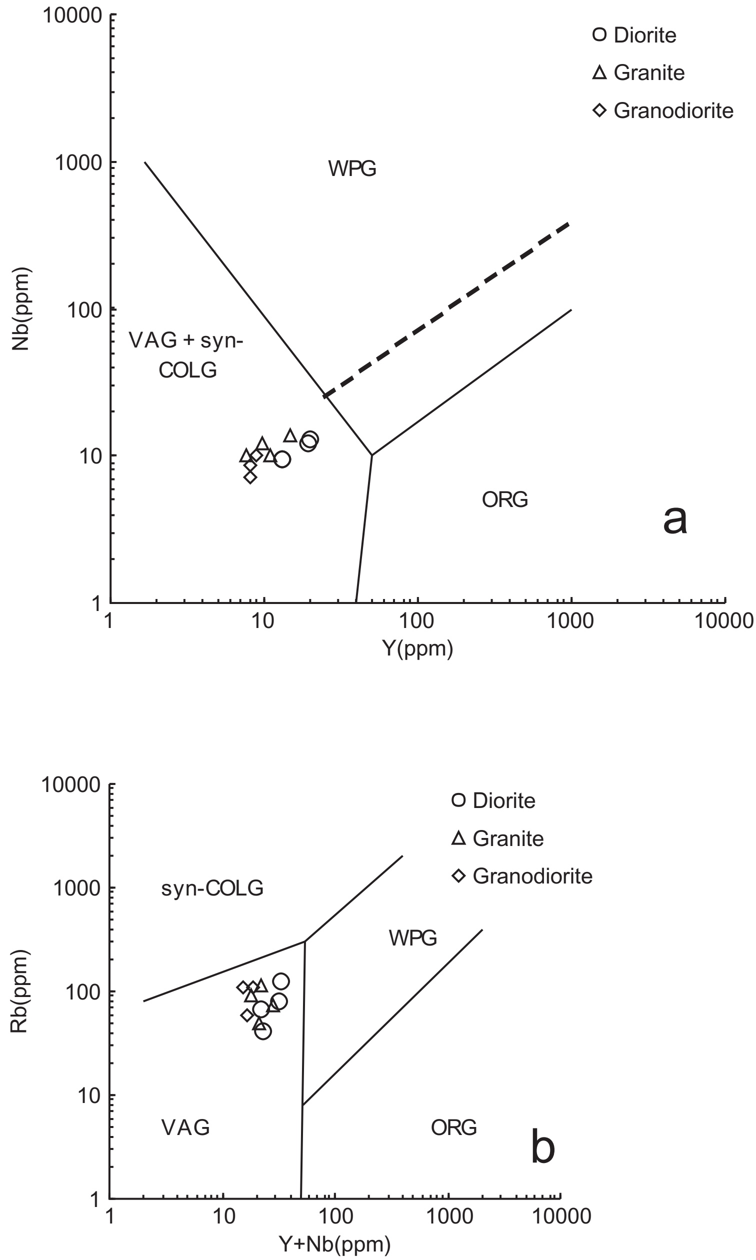

Figure 13. Tectonic environmental discriminations by trace elements of (a) Y versus Nb and (b) Y + Nb versus Rb of granitoid samples in the Zhangbaling Belt (after Pearce *et al.* 1984). VAG, volcanic arc granite; Syn-COLG, syn-collision granite; ORG, middle-ridge granite; WPG, within-plate granite.

systems. However, understanding of the sources of the metals and fluids remains ambiguous. Previous studies have suggested different sources of the fluids for the orogenic gold deposits, such as, hydrous fluids liberated by metamorphic dehydration (McCuaig and Kerrich 1998), magmatic-hydrothermal fluids (De Ronde *et al.* 2000), deeply convecting meteoric water (Jenkin *et al.* 1994), CO_2-rich fluids released from the mantle (Colvine 1989), or fluids from an external source (Breeding and Ague 2002). Meanwhile, the orogenic deposits usually display three mineralization stages (Chen *et al.* 2004c) and the isotopic compositions of the ore-forming fluids are generally variable for these stages (Chen *et al.* 2004b). Therefore, it is suggested that isotope indicators are not necessarily diagnostic in terms of metamorphic and magmatic sources of fluids and metals (Chen *et al.* 2004c). In addition to the sources of the metals and fluids, the orogen tectonic setting, structure-control of the orebodies, and CO_2-rich metamorphic fluid system are key markers of orogenic-type gold lodes (Chen *et al.* 2004c, 2005). Virtually all orogenic gold deposits show a close spatial association with 'first- and second-order' structural breaks (Bierlein *et al.* 2004). All these 'necessarily diagnostic indicators' and 'virtual characters' are evidently shown in the gold deposits in the ZTB.

Comparison with gold deposits in Jiaodong

Jiaodong gold metallogenic zone is a famous gold-centralized area in China, which is adjacent to the Tan-Lu fault zone to the W, the same as the ZTB. The strata in the belt are composed of the Archaean Jiaodong Group, Proterozoic Jinshan Group, Fenzishan Group, and Penglai Group. The Mesozoic granitoids, such as Linglong granite, Guojiazhai granodiorite, Lanjiahe granite, and Kunlunshan granite, are widely developed in the region. Wang *et al.* (1998) obtained the zircon SHRIMP dating result of 150–160 Ma from Linglong granite. The $^{40}Ar/^{39}Ar$ step-heating ages of the biotite from Guojiazhai granodiorite are 124.0 ± 0.4 to 124.5 ± 0.4 Ma (Li *et al.* 2003). The dating results suggest that Mesozoic granitoids in Jiaodong were emplaced during several thermal events. The identification of inherited zircons coupled with I_{Sr} ratios (>0.709) indicate that these granitoids were mainly derived from the continental crust by re-melting or partial melting (Chen *et al.* 2007a).

The gold deposits in Jiaodong are controlled by fractures mainly in NNE striking, which were considered as derivative structures of the Tan-Lu fault zone (Goldfarb *et al.* 2001; Zhou *et al.* 2002). Three types of gold deposits, altered-tectonite gold deposits, quartz-vein gold deposits, and hydrothermal breccia gold deposits, can be identified in the region (Mao *et al.* 2005). Based on the dating combined with the analysis of previous data, Chen *et al.* (2004a, 2007b) suggested that in the Jiaodong gold province, mineralization occurred in the Mesozoic, with peak activities between 110 and 130 Ma, coeval with or postdating Mesozoic granitoid intrusions. The I_{Sr} values obtained from ores and fluid inclusions are generally higher than 0.709 and slightly higher than those from Mesozoic granitoids, which indicates that both ore fluids and metals were mainly derived from the crust (Chen *et al.* 2004b, 2007a). The granitoid emplacement and large-scale gold metallogenesis were related to three evolution stages in a collisional orogen, and the most important metallogenic phase occurred at the transition from collisional compression to extension (Chen *et al.* 2004a, 2007b). From the discussion above, it can be seen that the gold deposits in the ZTB are very similar to those in the Jiaodong gold metallogenic province in the tectonic settings, mineralization-controlling factors, and mineralization ages, as well as in the ore-forming temperature and the oxygen and hydrogen isotopes composition to some extent, which convince us of an orogenic origin for the gold deposit in ZTB.

Comparison with deposits in Xiongershan

Xiaoqinling-Xiong'ershan in East Qinling is another important base of gold and other metals in China. Some of the gold deposits in this area are considered to be orogenic

(Chen *et al.* 2004c). The Shanggong gold deposit can be taken as the typical representation of orogenic gold deposits in this belt. The Shanggong gold deposit is located in Xiong'ershan terrane, which is in the northern part of Qingling-Dabie orogen. The strata distributing in this terrane mainly include Archaean Taihua Group and Middle Proterozoic Xionger Group. The former mainly consists of gneiss and hornblendite and the later of basalt, basaltic andesite, andesite, dacite, and rhyolite (Chen *et al.* 2004c). The Mesozoic granitoids, such as Haopinggou granite, Wuzhangshan granodiorite, and Huashan granite, are developed in this region.

The mineralization is controlled by fractures mainly in NE striking, which were considered to have evolved from compressional shear to tensional shear (Chen *et al.* 2004c). The hydrothermal ore-forming process is divided into early, middle, and late stages, characterized by pyrite-ankerite-quartz, polymetallic sulphides, and carbonate-quartz, respectively. The early-stage veins and minerals are structurally deformed and broken, suggesting that they are formed in a compression or compressional shear setting. The middle stage (polymetallic sulphide stage) shows no clear deformation, which suggests a tensional shear setting. The late stage, characterized by developed quartz-carbonate veinlets and comb structure, is likely formed in an extensional tectonic environment (Chen *et al.* 2004c). T_h are between 380–320°C for the early stage, 300–220°C for the middle stage, and 120–200°C for the late stage (Chen *et al.* 2004c).

The $\delta^{18}O$ and δD values of the ore-forming fluids are: 4.2–13.4‰ and −66–88‰ for the early stage, 1.9–4.5‰ and −1.2–0.5‰, for middle stage, and −2.0–0.6‰ and −56‰ for late stage (Chen *et al.* 2004b). The $\delta^{18}O$ and δD values of the fluids from the deposits in the Zhangbaling area can be compared with the middle- and late-stages ore-forming fluids in the Shanggong gold deposit. The age, obtained by the $^{40}Ar/^{39}Ar$ dating, of the early stage is 222.8 Ma ± 24.9 Ma. Rb/Sr isochron dating for sericite, calcite, and quartz or altered rocks formed in the early, middle, and late stages yield ages of 242 Ma ± 10 Ma, 165 Ma ± 7 Ma, and 113 Ma ± 6 Ma, respectively. This implies that the gold mineralization occurred in the period of 250–100 Ma, and was coeval with the continent–continent collision between the Yangtze and North China plates (Chen *et al.* 2004d), which shows a similar situation to that in the ZTB.

By comparing the famous gold deposits in Jiaodong and Xiong'ershan in China, we proposed that the gold deposits in the ZTB are probably orogenic gold deposit and this region is rather favourable for further exploration of gold resource.

Conclusions

Two types of gold deposits, altered-tectonite and quartz-vein, were developed in the ZTB during the Yanshanian period. It is evident that the gold mineralization, either from deposit or orebody scale, was controlled by fractures. The mineralization processes include early, middle, and late stages for both types of deposits. The T_h of three stages were 115–165°C, 235–275°C, and 335–395°C for altered-tectonite gold deposits, and 145–195°C, 205–255°C, and 255–335°C for quartz-vein gold deposits, respectively. The D–O isotope analyses indicate that the ore-forming fluids of quartz-vein gold deposits had two sources: Mesozoic meteoric water and magmatic water. The ore-forming elements of gold deposits were derived mainly from the Yanshanian granites, which originated from melting of the lower crust during or slightly post-orogeny. The gold deposits in the ZTB are remarkably similar to those in the Jiaodong gold metallogenic province and in the Xiong'ershan metallogenic zone with regard to tectonic settings, mineralization-controlling factors, and mineralization ages, as well as the ore-forming temperatures and the O–D isotopes compositions. We suggest that the gold deposits in the ZTB are probably orogenic gold deposits similar to those in the Jiaodong and the Xiong'ershan. This conclusion suggests that the ZTB is a favourable target for further exploration of gold resources.

Acknowledgements

This study is supported by Bureau of Geology and Mineral Resources of Anhui Province, the National Natural Science Foundation of China (No. 90814008), and the Opening Foundation of State Key Laboratory of Ore Deposit Geochemistry, Institute of Geochemistry, CAS (No. 2008011). The fluid inclusions microthermometric measurement and isotopes and REE analyses were conducted by Yichang Institute of Geology and Resources. The authors specially thank Dr H.Y. Chen and Professor Y.J. Chen for many useful comments and corrections.

References

BGMR (Bureau of Geology and Mineral Resources of Anhui Province), 1987, Regional geology of Anhui province: Beijing, Geological Publishing House (in Chinese).

Bierlein, F.P., Christie, A.B., and Smith, P.K., 2004, A comparison of orogenic gold mineralisation in central Victoria (AUS), western South Island (NZ) and Nova Scotia (CAN): Implications for variations in the endowment of Palaeozoic metamorphic terrains: Ore Geology Reviews, v. 25, p. 125–168.

Breeding, C.M., and Ague, J.J., 2002, Slab-derived fluids and quartz vein formation in an accretionary prism, Otago schist, New Zealand: Geology, v. 30, p. 499–502.

Chen, Y.J., Chen, H.Y., Zaw, K., Pirajno, F., and Zhang, Z.J., 2007b, Geodynamic settings and tectonic model of skarn gold deposits in China: An overview: Ore Geology Reviews, v. 31, p. 139–169.

Chen, Y.J., Lin, Z.J., Pirajno, F., Li, J., Lin, Z.J., and Wang, H.H., 2004c, Hydrothermal metallogy of the Shanggong gold deposit, East Qinling: study on the ore geology and fluid inclusion geochemistry: Journal of Mineralogy and Petrology, v. 24, no. 3, p. 1–12 (in Chinese with Englsih abstract).

Chen, Y.J., Lin, Z.J., Pirajno, F., Li, J., and Wang, H.H., 2004b, Hydrothermal metallogy of the Shanggong gold deposit, East Qinling: study on the isotope geochemistry: Journal of Mineralogy and Petrology, v. 24, no. 3, p. 13–21 (in Chinese with Englsih abstract).

Chen, Y.J., Ni, P., Fan, H.R., Pirajno, F., Lai, Y., Su, W.C., and Zhang, H., 2007a, Diagnostoc fluid inclusions of different types hydrothermal gold deposits: Acta Petrologica Sinica, v. 23, no. 9, p. 22088–22108 (in Chinese with English abstract).

Chen, Y.J., Pirajno, F., Lai, Y., and Li, C., 2004a, Metallogenic time and tectonic setting of the Jiaodong gold province, eastern China: Acta Petrologica Sinica, v. 20, no. 4, p. 907–922 (in Chinese with English abstract).

Chen, Y.J., Pirajno, F., and Qi, J.P., 2005, Origin of gold metallogeny and sources of ore-forming fluids, in the Jiaodong province, eastern China: International Geology Review, v. 47, p. 530–549.

Chen, Y.J., Tang, G.J., Pirajno, F., Qi, J.P., and Lin, Z.J., 2004d, Hydrothermal metallogy of the Shanggong gold deposit, East Qinling: radiogenic isotope geochemistry: Journal of Mineralogy and Petrology, v. 24, no. 3, p. 2–27 (in Chinese with English abstract).

Colvine, A.C., 1989, An empirical model for the formation of Archean gold deposits: products of final cratonization of the Superior province, Canada: Economic Geology, v. 6, p. 37–53.

De Ronde, C.E.J., Faure, K., Bray, C.J., and Whitford, D.J., 2000, Round Hill shear zone-hosted gold deposit, Macraes flat, Otago, New Zealand: Evidence of a magmatic ore fluid: Economic Geology, v. 95, p. 1025–1048.

Dong, S.W., and Huang, D.Z., 1995, The tectonic map of Lower and Middle Yangtze River and the adjacent area (1:1000000): Interior data of Bureau of Geology and Mineral Resources of Anhui Province, China: Hefei (in Chinese).

Goldfarb, R.J., Groves, D.I., and Gardoll, S., 2001, Orogenic gold and geological time: A global synthesis: Ore Geological Reviews, v. 18, p. 1–73.

Hou, M.J., Wu, Y.D., and Tang, J.F., 2004, Mid-upper crust deformation features of the Dabie orogenic belt: Studies on Indosinia to early Yanshanian deformation in the Zhangbaling region, central China: China Journal of Geology, v. 31, no. 2, p. 123–130 (in Chinese with English abstract).

Huang, D.Z., Qiu, R.L., Liu, D.L., and Yang, X.Y., 2000b, Verification of the Guandian-Longwangjian Fault and TEM analysis of mylonites and its geological significance: Geological Review, v. 46, no. 1, p. 58–63 (in Chinese with English abstract).

Huang, D.Z., Qiu, R.L., Liu, D.L., Yang, X.Y., and Xu, X., 2000a, Study on the origin of ore-forming fluids of quartz-vein-type gold deposits in Zhangbaling Tectonic Belt, Anhui: Geotectonica et Metallogenia, v. 24, no. 3, p. 231–236 (in Chinese with English abstract).

Jenkin, G.R.T., Craw, D., and Fallick, A.E., 1994, Stable isotopic and fluid inclusion evidence for meteoric fluid penetration into an active mountain belt: Alpine schist, NewZealand: Journal of Metamorphic Geology, v. 12, p. 429–444.

Jin, Y.R., Liang, W.T., Zhang, S.Y., and Zhang, L.T., 1991, Precambrian high-pressure belts of Anhui Province: Beijing: Geological Publish House, (in Chinese).

Lan, X.H., Yang, X.Y., Yu, L.F., Chi, Y.Y., and Zhang, Q.M., 2009, Geochemical studies on Shaxi porphyry copper-gold deposit: A clue to plate subduction of West Pacifi: Chinese Journal of Geochemistry, v. 28, no. 1, p. 28–43.

Le Maitre, R.W., Bateman, P., Dudek, A., Keller, J., Lameyre, J., Le Bas, M.J., Sabine, P.A., Schmid, R., Sorensen, H., Streckeisen, A., Wooley, A.R., and Zanettin, B., 1989, A classification of igneous rocks and glossary of terms: Oxford, Blackwell.

Li, J.W.J., Vasconcelos, P.M., Zhang, J., Zhou, M.F., Zhang, X.J., Yang, F.H., 2003, $^{40}Ar/^{39}Ar$ constraints on a temporal link between gold mineralization, magmat-ism, and continental margin transtension in the Jiaodong gold province, eastern China: Journal of Geology, v. 111, no. 6, p. 741–751.

Li, X.M., Li, B.X., Zhang, X., and Zhou, T.X., 1985, Isotopic ages of the Guandian intrusion in Anhui and dynamic metamorphism of the Tan-Lu fault zone: Journal of China University of Science and Technology, (Suppl.), v. 16, p. 254–261 (in Chinese with English abstract).

Liu, G.S., Zhu, G., Wang, D.X., Song, C.Z., and Niu, M.L., 2002, Strike-slip movement on Zhangbaling uplift segment of Tan-Lu fault and the depositional response in Hefei Basin: Acta Sedimentological Sinica, v. 20, no. 2, p. 267–273 (in Chinese with English abstract).

Lu, H.Z., Yuan, W.C., Zhang, G.P., Li, Y.S., and Long, H.B., 1999, Stable isotopes studies and age dating of gold deposits and Linglong granites in Linglong-Jiaodong area, Shandong, China: Journal of Guilin Institute of Technology, v. 19, no. 1, p. 1–8 (in Chinese with English abstract).

Mao, J.W., He, Y., and Ding, T.P., 2002, Mantle fluids involved in metallogenesis of Jiaodong (east Shandong) gold district: Evidence of C, O and H Isotopes: Mineral Deposits, v. 21, no. 2, p. 121–128 (in Chinese with English abstract).

Mao, J.W., Li, H.M., Wang, Y.T., Zhang, C.Q., and Wang, R.Y., 2005, The relationship between mantle-derived fluid and gold ore-formation in the eastern Shandong peninsula: Evidences from D-O-C-S Isotopes: Acta Geologica Sinica, v. 79, no. 6, p. 839–857 (in Chinese with English abstract).

Mao, J.W., Wang, Y.T., Lehmann, B., Yu, J.J., Du, A.D., Mei, Y.X., Li, Y.F., Zang, W.S., Stein, H.J., and Zhou, T.F., 2006, Molybdenite Re–Os and albite Ar-40/Ar-39 dating of Cu–Au–Mo and magnetite porphyry systems in the Yangtze River valley and metallogenic implications: Ore Geology Reviews, v. 29, p. 307–324.

McCuaig, T.C., and Kerrich, R., 1998, P-T-t deformation-fluid characteristics of lode gold deposits: Evidence from alteration systematic: Ore Geology Reviews, v. 12, p. 381–345.

Mercier, J.L., Hou, M.J., Vergély, P., and Wang, Y.M., 2007, Structural and stratigraphical constraints on the kinematics history of the Southern Tan–Lu Fault Zone during the Mesozoic Anhui Province, China: Tectonophysics, v. 439, no. 1–4, p. 33–66.

Naden, J., Kilias, S.P., Leng, M.J., Cheliotis, I., and Shepherd, T.J., 2003, Do fluid inclusions preserve $\delta^{18}O$ values of hydrothermal fluids in epithermal systems over geological time? Evidence from paleo- and modern geothermal systems, Milos island, Aegean Sea: Chemical Geology, v. 197, no. 1–4, p. 143–159.

Niu, B.G., Fu, Y.L., Liu, Z.G., and Ren, J.S., 1993, The $^{40}Ar/^{39}Ar$ Dating of blueschist in northern Hubei Province and its geological significance: Chinese Science Bulletin, v. 38, no. 4, p. 1309–1313 (in Chinese).

Niu, M.L., 2006, ^{40}Ar-^{39}Ar dating of biotites from the Mesozoic intrusions Zhangbaling area and its geological significance: Chinese Journal of Geology, v. 41, no. 2, p. 217–225 (in Chinese with English abstract).

Niu, M.L., Zhu, G., Liu, G.S., Wang, D.X., and Song, C.Z., 2002, Tectonic setting and deep processes of Mesozoic magmatism in middle-south segment of the Tan-Lu fault: Chinese Journal of Geology, v. 37, no. 4, p. 393–404 (in Chinese with English abstract).

Niu, M.L., Zhu, G., Xie, C.L., Liu, X.M., Cao, Y., and Xie, Y.W., 2008, LA-ICP MS zircon U–Pb ages of the granites from the southern segment of Zhangbaling uplift along the Tan-Lu fault zone and their tectonic significance: Acta Petrologica Sinica, v. 24, no. 8, p. 1839–1847 (in Chinese with English abstract).

O'Reilly, C., Jenkin, G.R.T., Feely, M., Alderton, D.H.M., and Fallick, A.E., 1997, A fluid inclusion and stable isotope study of fluid evolution in the Galway Granite, Connemara, Ireland: Contributions to Mineralogy and Petrology, v. 129, no. 1, p. 120–142.

Pearce, J.A., Harris, N.B.W., and Tindle, A.G., 1984, Trace element discrimination diagrams for the tectonic interpretation of granitic rocks: Journal of Petrology, v. 25, p. 956–983.

Qiu, Y.M., Groves, D.I., and McNaughton, N.J., 2002, Nature, age and tectonic setIing of granitoid-hosted, orogenic gold deposits of the Jiaodong Peninsula, eastern North China craton, China: Mineralium Deposita, v. 37, p. 283–305.

Rickwood, P.C., 1989, Boundary lines within petrologic diagrams which use oxides of major and minor elements: Lithos, v. 22, p. 247–263.

Shelton, K.L., and Lofstro, M., 1988, Stable isotope and fluid inclusion studies of W–Sn–Ag deposits, Silver Mine district, southeastern Missouri: Tectonic control of water-rock interaction in a magma tic hydrothermal system, *in*: Kisvarsanyi, G., and Grant, S.K., eds., Proceedings Volume. North America conference on tectonic control of ore deposit and the vertical and horizontal extent of ore system: Rolla, MO, University of Missouri-Rolla.

Sheppard, S.M.F., 1986, Characterization and isotopic variations in natural waters, *in* Valley, J.W., Taylor, H.P., Jr., and O'Neil, J.R., eds. Stable isotopes in high temperature geological processes: Reviews in Mineralogy, v. 16, no. 1, p. 165–184.

Shepherd, T.J., Rankin, A.M., and Alderton, D.H.M., 1985, A practical guide to fluid inclusion studies: Blackie, London.

So, C.-S., Choi, S.-H., and Shelton, K.L., 1997, Geochemistry and genesis of hydrothermal Cu deposit in the Gyeongsang Basin (Andong area), Korea: A link between porphyry and epithermal systems: Neues Jahrbuch für Mineralogie (Abh.), v. 171, p. 281–307.

Sun, W.D., Ding, X., Hu, Y.H., and Li, X.H., 2007, The golden transformation of the Cretaceous plate subduction in the west Pacific: Earth Planet Science Letters, v. 262, p. 533–542.

Wang, L.G., Qiu, Y.M., McNaughton, N.J., Groves, D.I., Luo, Z.K., and Huang, J.Z., 1998, Constraints on crustal evolution and metallogeny in the Northwestern Jiaodong Penisula, China: From SHRIMP zircon studies of granitoids: Ore Geology Reviews, v. 13, p. 275–291.

Wilkinson, J.J., Jenkin, G.R.T., Fallick, A.E., and Foster, R.P., 1995, Oxygen and hydrogen isotopic evolution of Variscan crustal fluids, south Cornwall, UK: Chemical Geology, v. 123, no. 1–4, p. 239–254.

Wilson, M., 1989, Igneous petrogenesis: London, Allen and Unwin.

Xiao, Q.H., Deng, J.F., and Ma, D.Q., 2002, The ways of investigation on granitoids: Beijing, Geological Publishing House.

Xie, J.C., Yang, X.Y., Sun, W.D., Du, J.G., Xu, W., Wu, L.B., Wang, K.Y., and Du, X.W., 2009, Geochronological and geochemical constraints on formation of the Tongling metal deposits, middle Yangtze metallogenic belt, east-central China: International Geology Review, v. 51, no. 5, p. 422–455.

Xu, G.Z., Ying, H.L., Zhou, R., She, H.Q., Yan, Z., Wang, Y.F., and Li, B., 2002, Genesis and dynamic condition of Hexi Gold Deposit in northwest Jiaodong area: Mineral Deposits, v. 21, no. 3, p. 246–255 (in Chinese with English abstract).

Xu, J.W., Zhu, G., Tong, W.X., Cui, K.R., and Liu, Q., 1987, Formation and evolution of the Tancheng-Lujiang wrench fault system, a major shear system to the northwest of the Pacific Ocean: Tectonophysics, v. 134, p. 273–310.

Yang, J.H., and Zhou, X.H., 2000, The Rb-Sr isochron of ore and pyrite subsamples from Linglong gold deposit, Jiaodong Peninsula, eastern China and their geological significance: Chinese Science Bulletin, v. 45, no. 24, p. 2272–2276.

Yang, X.-Y., Liu, D.L., Yang, X.-M., Wang, K., and Dai, J., 1998, Characteristics of compositional migration in mylonites from the ductile shear zones of the southern Tancheng-Lujiang (Tan-Lu) fault belt, Eastern Anhui Province: Acta Geologica Sinica, v. 72, p. 37–50.

Yang, X.Y., Liu, D.L., and Wagner, G.A., 2001a, Conditions of deformation and variations of compositional and structural state of feldspars during mylonitizaton: Exemplified from the ductile shear zones in south Tan-Lu fault belt of China: Neues Jahrbuch für Mineralogie (Mon.), v. jg2001, nos. 9–10, p. 415–432.

Yang, X.Y., Wang, K.R., Yang, X.M., and Sun, L.G., 2002, Characteristics of mineralization and gold occurrence in Shaxi porphyry copper-gold deposit, central Anhui, China: Neues Jahrbuch für Mineralogie (Abh), v. 177, p. 293–320.
Yang, X.Y., Yang, X.M., Zhang, Z.W., Chi, Y.Y., Yue, L.F., and Zhang, J.M., 2011, A porphyritic copper (gold) ore-forming model for the Shaxi-Changpushan district, Lower Yangtze metallogenic belt, China: Geological and geochemical constraints: International Geology Review, v. 53, p. 580–611.
Yang, X.Y., Zheng, Y.F., Liu, D.L., and Dai, J.X., 2001b. Study on chemical compositions of fluid inclusions from peridotite and eclogites in Eastern China: The geodynamic implications: Physics and Chemistry of the Earth, v. 26, p. 705–718.
Yang, X.Y., Zheng, Y.F., Xiao, Y.-L., Du, J.-G., and Sun, W.-D., 2007, $^{40}Ar/^{39}Ar$ dating of Shaxi porphyry Cu–Au deposit, South Tancheng-Lujiang fault belt, Anhui Province: Acta Geologica Sinica, v. 76, no. 3, p. 801–812.
Ying, H.L., and Liu, B.G., 2002, $^{40}Ar–^{39}Ar$ dating of gold-bearing quartz vein in Fengyang and Zhangbaling areas, Anhui Province, and its geological significance: Mineral Deposits, v. 21, no. 3, p. 240–245 (in Chinese with English abstract).
Zhang, L.G., 1989, Petrogentic and minerogenitic theories and prospecting: Beijing, China, Press of University of Technology.
Zhang, Z.Q., Lai, Y., and Chen, Y.J., 2007, Fluid inclusion study of the Linglong gold deposit, Shandong province, China: Acta Petrologica Sinica, v. 23, no. 9, p. 2207–2216 (in Chinese with English abstract).
Zhang, Z.Q., Zhu, G., Liu, G.S., Teyssierl, C., and Dunlap, W.J., 2008, Sinistral transpressive deformation in the northern part of Zhangbaling uplift in the Tan-Lu fault zone and its $^{40}Ar/^{39}Ar$ dating: The Science Frontiers, v. 15, no. 3, p. 34–249 (in Chinese with English abstract).
Zhou, T.H., Goldfarb, R.J., and Phillips, G.N., 2002, Tectonics and distribution of gold deposits in China: an overview: Mineralium Deposita, v. 37, p. 249–282.
Zhu, D.Y., Zhang, J.F., Huang, S.Q., and Li, G.M., 2007, The controlling of the fractures on the gold deposits in Jiashan-Guandian area, Symposium of Mineral: Lithology and Geochemistry of Hunan: Changsha, Press of Central South University, p. 220–223.
Zhu, G., Song, C.Z., Wang, D.X., Liu, G.S., and Xu, J.W., 2001a, $^{40}Ar/^{39}Ar$ geochronologic studies on the strike-slip time of the Tan-Lu fault zone and its tectonic implication: Science in China (Series D), v. 31, no. 3, p. 250–255 (in Chinese with English abstract).
Zhu, G., Wang, D.X., Liu, G.S., Song, C.Z., Xu, J.W., and Niu, M.L., 2001b, Extensional activities along the Tan-Lu fault and its geodynamic setting: Chinese Journal of Geology, v. 36, no. 3, p. 269–278 (in Chinese with English abstract).